Acta Pharmaceutica Sinica B 2026;16(8):5351−5362

Chinese Pharmaceutical Association
Institute of Materia Medica, Chinese Academy of Medical Sciences

Acta Pharmaceutica Sinica B

www.elsevier.com/locate/apsb
www.sciencedirect.com

ORIGINAL ARTICLE

Design, preclinical evaluation, and multicenter phase 1 clinical study of HZ-A-018 for relapsed or refractory central nervous system lymphoma

Shenglan Li[a,†], Jialiang Lu[b,f,†], Zhuang Kang[a,†], Haiyan Yang[c], Wenbin Qian[d], Xi Chen[c], Xianggui Yuan[d], Miao Hu[e], Qiuqiu Shi[b,f], Xinglu Zhou[e], Feng Chen[a,*], Xiaowu Dong[b,f,*], Wenbin Li[a,*]

[a]*Cancer Center, Beijing Tiantan Hospital, Capital Medical University, Beijing 100070, China*
[b]*College of Pharmaceutical Sciences, Zhejiang University, Hangzhou 310058, China*
[c]*Department of Lymphoma, Zhejiang Cancer Hospital, Hangzhou 310022, China*
[d]*Department of Hematology, The Second Affiliated Hospital, Zhejiang University School of Medicine, Hangzhou 310009, China*
[e]*HealZen Therapeutics Co., Ltd., Hangzhou 310018, China*
[f]*ZJUCPS-HealZen Joint Laboratory of Drug Innovation and Transformation, Zhejiang University, Hangzhou 310058, China*

Received 13 August 2025; received in revised form 26 January 2026; accepted 14 April 2026

KEY WORDS

Bruton tyrosine kinase;
Central nervous system lymphoma;
BTK inhibitors;
HZ-A-018;
Blood−brain barrier;
BBB permeability;
Phase 1 clinical trial;
AI-driven drug discovery

Abstract Effective therapy for relapsed or refractory central nervous system lymphoma (r/r CNSL) remains an unmet medical need. Meanwhile, developing antitumor drugs for CNS malignancies faces the dual challenge of achieving effective blood−brain barrier (BBB) penetration and potent tumor cell killing. To address these challenges, a comprehensive predictive system was established to support decision-making during the discovery of HZ-A-018, a potent and BBB-permeable Bruton tyrosine kinase (BTK) inhibitor. This study further presents key preclinical results for HZ-A-018, as well as efficacy/safety data from a multicenter Phase 1 trial in r/r CNSL patients. HZ-A-018 demonstrated manageable safety, with only 19.2% of patients experienced grade 3 or higher adverse events according to the Common Terminology Criteria for Adverse Events version 5.0. Treatment with HZ-A-018 at the recommended phase II dose (RP2D) of 600 mg achieved an overall response rate (ORR) of 72.7% (95% CI, 39.0−94.0) and a 12-month survival rate of 90.5%. The Center for Drug Evaluation in China has authorized the initiation of this single-arm Phase II study as a pivotal registrational clinical trial for accelerated

*Corresponding authors.
E-mail addresses: chenfeng406@sina.com (Feng Chen), dongxw@zju.edu.cn (Xiaowu Dong), liwenbin@ccmu.edu.cn (Wenbin Li).
[†]These authors made equal contributions to this work.

Peer review under the responsibility of Chinese Pharmaceutical Association and Institute of Materia Medica, Chinese Academy of Medical Sciences.

https://doi.org/10.1016/j.apsb.2026.05.021

approval of HZ-A-018 for monotherapy in patients with r/r PCNSL. This trial has been registered under the identifiers ChiCTR2400091821 at www.chictr.org.cn and CTR20210181 at www.chinadrugtrials.org.cn.

1. Introduction

Primary central nervous system lymphoma (PCNSL) is an aggressive extranodal non-Hodgkin lymphoma that is characterized by a short course of the disease, rapid progression, and poor prognosis with a 5-year survival rate typically ranging from about 22% to 40%[1−5]. Secondary central nervous system lymphoma (SCNSL) occurs in a subset of patients with diffuse large B-cell lymphoma (DLBCL), with an inferior prognosis and a median survival of only 2−6 months [6−8]. The standard of care for relapsed or refractory central nervous system lymphoma (r/r CNSL) has yet to be established [9,10].

Although bruton tyrosine kinase (BTK) inhibitors ibrutinib and tirabrutinib have shown specific efficacy in treating r/r PCNSL, ibrutinib may cause toxicities arising from inhibition of structurally related kinases, and tirabrutinib is associated with a higher proportion of patients who had a grade ≥3 adverse event (AE) (47.7%) [11,12]. Consequently, CNS drug discovery−particularly for r/r CNSL−faces formidable barriers: remaining clinical gaps, a limited repertoire of inhibitors whose optimization potential remains underexplored. In particular, enhancing drug permeability across the blood−brain barrier (BBB) while maintaining their antitumor efficacy is a critical challenge [13,14]. Fortunately, with the accumulation of biomedical data, advancements in computational capabilities, and ongoing algorithm refinement, artificial intelligence (AI) has emerged as an indispensable tool for deriving meaningful insights and enhancing decision-making in central nervous system drug discovery[15−20]. Nevertheless, there is still a lack of comprehensive AI models that could simultaneously predict both BBB permeability and antitumor efficacy of compounds, thereby limiting rapid drug discovery in CNSL to some extent.

Therefore, this study focuses on the development of a system with dual prediction capabilities for compound brain penetration and tumor cell killing capacity, followed by drug synthesis and characterization, preclinical studies, and clinical studies. Specifically, we describe the discovery, preclinical evaluation, and a multicenter phase 1 clinical study of HZ-A-018, an oral BTK inhibitor with BBB permeability, identified through a discovery platform combining BTK inhibition prediction with a Graph Attention Network-based BBB permeability prediction. Furthermore, we initiate preclinical experiments to evaluate the brain penetration and tumor cell killing properties of HZ-A-018, and a phase Ia clinical trial to evaluate the safety, preliminary efficacy, and pharmacokinetic profile of HZ-A-018 in patients with r/r CNSL.

2. Materials and methods

2.1. BTK inhibition activity and BBB permeability prediction model

The BTK inhibition activity dataset was obtained from the ChEMBL API (Uniprot ID Q06187), and IC_{50} values were converted to pIC_{50} for data consistency. After removing salts and duplicate SMILES, the unique SMILES structures and their associated properties were compiled into the final dataset. KnoMol (https://github.com/gaojianl/KnoMol [20]), the model used in this study, combines a graph neural network and a Transformer architecture, with its attention mechanisms enhanced by incorporating knowledge graphs. Hyperparameter optimization was performed using Hyperopt, and training was run for a specified number of epochs. Model performance was assessed on the validation set. The hyperparameters and their respective search spaces were as follows: learning rate, sampled from a log-uniform distribution between 1e-5 and 1e-2; attention layers, sampled from 1 to 4; dropout rate, chosen from 0.05 to 0.1; and batch size, selected from 8, 32, and 256. After identifying the optimal hyperparameters, the model was retrained and evaluated on the test set (batch_size = 32, attn_layers = 2, lr = 0.01, dropout_rate = 0.05, output_dim = 256, D = 4, and seed = 426). The final model weight used for evaluation was *BTK_C2reg_2_1.2517999410629272. pkl*. Furthermore, the BBB dataset was obtained from https://github.com/theochem/B3DB. The model employed in this study was KnoMol, with the hyperparameter search range identical to that of the BTK inhibition activity dataset prediction model. After identifying the optimal hyperparameters, the model was retrained and subsequently evaluated on the test set (numtasks = 1, batch_size = 32, attn_layers = 4, lr = 0.01, dropout rate = 0.05, output_dim = 128, D = 2, and seed = 426). The final model weight used for evaluation was *B3DB_regression_C2reg_48_0.4975000023841858. pkl.*

2.2. Molecular docking and dynamics simulation

Covalent docking of HZ-A-018 was performed with default parameters, and the best-scoring conformation was selected for subsequent covalent molecular dynamics simulations. The complex was solvated in a TIP3P water box, and simulations were carried out in the NPT ensemble (300.0 K, 1.01325 bar) for 50 ns, with trajectories saved every 100 ps. Root-mean-square deviation (RMSD) values and covalent protein−ligand interactions were then analyzed over the course of the trajectories.

2.3. Cellular BTK occupancy assay

The occupancy of BTK by HZ-A-018 in primary human peripheral blood mononuclear cells (PBMCs) was assessed using a biotinylated probe-based competition ELISA. Briefly, human PBMCs were isolated from fresh heparin-anticoagulated blood using standard density-gradient centrifugation. Cells were resuspended in assay medium (RPMI-1640 supplemented with 10% fetal bovine serum) and seeded into a 96-well plate at a density of 2×10^6 cells per well. Cells were then treated with a serial dilution of HZ-A-018 or a vehicle (DMSO) and incubated at 37 °C

under 5% CO_2 for 1 h to allow for target engagement. After washing, unoccupied BTK was labeled by incubating cells with 1 μmol/L HZ-A-018-biotin probe. Cells were lysed, and the lysates, along with a biotinylated BTK standard, were captured on streptavidin-coated plates. Captured BTK was detected using an anti-BTK primary antibody (1:1000 dilution in PBS with 0.5% BSA) and an HRP-conjugated secondary antibody, followed by TMB substrate development. The concentration of free BTK was determined from the standard curve, and BTK occupancy was calculated based on the decrease in free BTK compared with the total BTK level.

2.4. Cell culture

OCI-LY10 cells were obtained from the American Type Culture Collection (ATCC) (Manassas, VA, USA) and maintained at 37 °C in Iscove's modified Dulbecco's medium supplemented with 20% fetal bovine serum (FBS) (GIBCO) and 100 U/mL penicillin and 100 μg/mL streptomycin. The SU-DHL-6, WSU-DLCL2, and Mino cell lines were also obtained from ATCC and cultured in RPMI-1640 medium supplemented with 10% FBS, 100 U/mL penicillin, and 100 μg/mL streptomycin (Invitrogen, USA). The TMD8 cell line was provided by Dr. Yubo Zhou (Shanghai Institute of Materia Medica, Chinese Academy of Sciences) and cultured in RPMI-1640 medium supplemented with 10% FBS, 100 U/mL penicillin, and 100 μg/mL streptomycin (Invitrogen, USA). All cells were cultured at 37 °C under 5% CO_2. STR profiling was used to authenticate all cell lines, and the cells were routinely tested for mycoplasma contamination.

2.5. Cell viability assay

After drug incubation was complete, 20 μL of CellTiter 96® Aqueous Non-Radioactive Cell Proliferation Assay (MTS; Promega, Madison, WI) or 10 μL of Cell Counting Kit-8 (CCK8) solution was added to each well. The plates were then incubated at 37 °C for 1−4 h. Optical density was measured at 490 nm (background values measured at 690 nm were subtracted for MTS) or 450 nm (background values measured at 650 nm were subtracted for CCK8) using a SpectraMax 340 microplate reader (Molecular Devices, Sunnyvale, CA, USA). The activity was calculated using Eq. (1):

$$\text{Activity}\ (\%) = (OD_{Sample} - OD_{Blank})/(OD_{DMSO} - OD_{Blank}) \times 100 \quad (1)$$

A fitted curve was generated by nonlinear regression, and the IC_{50} was calculated using the GraphPad Prism software with the log (inhibitor) *vs* normalized response variable slope setting. Data are presented as mean ± SD from at least two independent assays performed in triplicate.

2.6. Western blot

Total proteins were extracted using RIPA lysis buffer (Beyotime, P0013B). A total of 40 μg of protein was separated to 12% SDS-PAGE and transferred to a PVDF membrane (Bio-Rad, Hercules, CA, USA). The membranes were blocked with 5% non-fat milk at room temperature for 1 h and then incubated with primary antibodies overnight at 4 °C. The primary antibodies used were as follows: *p*-BTK (87141, CST), BTK (8547, CST), ERK (4695, CST), p-ERK (4370, CST), PLCγ-2 (3872, CST), and p-PLCγ-2 (3871, CST). After washing with Tris-buffered saline with Tween 20, membranes were incubated with secondary antibodies at room temperature for another 1 h. The protein bands were visualized using the ECL detection system (WBKLS0050, EMD Millipore, Billerica, MA, USA) and analyzed using Bio-Rad Laboratories Quantity One software (Bio-Rad, Hercules, CA, USA).

2.7. Animal model construction

All animal studies were approved by the Institutional Animal Care and Use Committee of Zhejiang University (ZJU20241028), China. The Mino cells in the logarithmic growth phase were collected and resuspended in serum-free medium at 5×10^7 cells/mL before being placed on ice. The anesthetized mice (female CB17-SCID mice aged 4−5 weeks) were secured on a stereotaxic frame (David Kopf Instruments, Tujunga, CA, USA), and each mouse was intracranially inoculated with 2 μL of tumor cell suspension containing 10^5 cells/mouse to establish the brain tumor model. Specifically, a Hamilton syringe containing 2 μL of cell suspension was inserted into the brain at 2 mm to the right of the medial suture and 0.4 mm anterior to the bregma, to a depth of 3 mm, and held for 3 min. Subsequently, the syringe was retracted by 0.4 mm, and the cell suspension was infused at 667 nL/min for 3 min using a microinfusion pump. After infusion, the syringe was placed for another 2 min before being carefully withdrawn. The puncture site was sealed with bone wax, and the skin was sutured.

2.8. MDCK-MDR1

Sundia Biotechnology Co., Ltd. performed P-gp substrate evaluation of ibrutinib, tirabrutinib, and HZ-A-018 in MDCK-MDR1 cells.

2.9. Trial design and treatment

The HZ-A-018-102 study is an ongoing phase I/II trial evaluating the safety, tolerability, pharmacokinetics, and antitumor activity of HZ-A-018 in patients with CNSL. The study was designed with three distinct parts. (1) phase Ia monotherapy, comprising a dose escalation phase and a dose-expansion phase; (2) phase Ib combination therapy with high-dose methotrexate (HD-MTX); and (3) phase II monotherapy at the recommended phase II dose (RP2D) as a pivotal study (trial protocol, Supporting Information). Herein, we report the safety and efficacy outcomes from the phase Ia monotherapy of the study.

Phase Ia was an open-label, dose-escalation, and dose-expansion study designed to determine the safety/tolerability, and efficacy of HZ-A-018 in patients with r/r PCNSL, secondary CNS lymphoma (SCNSL), and primary vitreoretinal lymphoma (PVRL). The primary objective included safety, tolerability, and the recommended phase 2 dose (RP2D). The secondary objective included efficacy and pharmacokinetics. Efficacy endpoints included overall response rate (ORR), complete response rate (CRR), duration of response (DOR), progression-free survival (PFS), and overall survival (OS).

Patients were administered HZ-A-018 capsules once daily in 28-day cycles until disease progression or unacceptable toxicity. In the dose-escalation phase, HZ-A-018 was escalated from 300 mg QD to 450 mg QD, then to 600 mg QD, using the traditional "3 + 3" design. Dose-limiting toxicity (DLT) for each cohort was evaluated during the first 28-day cycle, with treatment

continuing until disease progression or emergence of clinically unacceptable toxicity.

A DLT was defined as treatment-related toxicity that includes any of the following: death, grade 4 hematologic toxicity, grade 3 febrile neutropenia, grade 3 thrombocytopenia with bleeding, nonhematologic toxicity of grade $\geq$3, and grade $\geq$3 diarrhea, nausea, or vomiting that persisted despite appropriate treatment. Patients who received at least 75% of their prescribed dose during cycle 1 (C1) or experienced a DLT during C1 were considered evaluable. The maximum tolerated dose (MTD) was defined as the highest dose at which no more than 33% of evaluable patients experienced a DLT.

In the dose escalation phase, up to six additional subjects could be enrolled in the above dose groups if fewer than one-third of the subjects experienced DLT and certain participants achieve at least PR, CRu, or CR in the dose group (DLT assessment was not required for these subjects). During the study, two dose levels (450 mg QD and 600 mg QD) were selected for dose expansion based on safety, PK, and efficacy results from the dose-escalation part after a protocol amendment.

In the phase Ia monotherapy trial, all patients provided informed consent before undergoing any study procedures. The protocol was approved by the Ethics Committee and the Center for Drug Evaluation (CDE) of China as part of an Investigational New Drug Application, in accordance with Good Clinical Practice and the principles outlined in the Declaration of Helsinki.

2.10. Patients

Patients diagnosed with PCNSL, PVRL, or SCNSL of B-cell type were enrolled in phase Ia monotherapy. Eligible Patients were required to have experienced relapse or refractory to at least one prior line of treatment. Specifically, PCNSL and SCNSL patients were required to have received at least one prior HD-MTX therapy, while patients with PVRL needed to have received at least one prior HD-MTX therapy or intraocular therapy. There were no restrictions on the number of recurrences. Patients with SCNSL actively receiving treatment for extra-CNS disease were excluded.

2.11. Assessments

Toxicity was assessed according to the Common Terminology Criteria for Adverse Events (AE) version 5.0. The relationship between AE and HZ-A-018 treatment was determined based on the investigator's assessment. Safety summaries included data from all patients who received at least one dose of HZ-A-018.

The therapeutic responses were evaluated using the International PCNSL Collaborative Group Response Criteria [21], and the assessment was performed at baseline using magnetic resonance imaging (MRI) and computed tomography (CT) scans of the chest, abdomen, and pelvis with contrast. For SCNSL patients, CT was substituted with positron emission tomography/CT (PET/CT) scans. Ophthalmological examinations were performed by ophthalmologists experienced in PVRL. The follow-up assessments were planned on Day 1 (D1) of Cycle 2 (C2), Cycle 3 (C3), Cycle 5 (C5), and subsequently on D1 every 8 weeks until disease progression or unacceptable toxicity.

Once a subject had received the last dose of study treatment, the subject moved into the survival follow-up period and was followed up every 8 weeks by clinic visit, telephone, or email.

For pharmacokinetic analyses, blood samples were collected immediately before drug administration, then at 20 min, 1, 2, 3, and 5 h after administration on D1 of C3. CSF samples were collected 2 h post-dose on D1 of C3. HZ-A-018 concentrations were determined using a validated liquid chromatography-mass spectrometry method. Key pharmacokinetic parameters included the maximum observed plasma concentration, the area under the plasma concentration-time curve, and the concentration of HZ-A-018 in CSF.

For exploratory analyses, DNA was extracted from archived tumor samples of the initial diagnostic brain biopsies. CSF was collected at baseline, C3D1, C5D1, and at disease progression to identify mutations, including *MYD88*, *CD79b*, and *CARD11*.

2.12. Statistical analysis

Descriptive statistics were used to summarize the findings in each defined cohort, including means, standard deviations, and medians for continuous variables and proportions for discrete variables. All analyses included patients who received at least one dose of the study drug. The ORR was calculated with a 95% confidence interval using the Clopper−Pearson method. Time-to-event analysis was conducted using the Kaplan−Meier method. Median follow-up was estimated using the reverse Kaplan−Meier method. PFS was defined as the time from initiating HZ-A-018 treatment to either disease progression or death from any cause. PFS duration was censored according to the following rules: 1) subjects without a baseline disease assessment were censored at the date of first dose; 2) subjects without documented PD or death before initiating a new antitumor therapy and before the end of the study were censored at the date of their last disease assessment; 3) subjects who were alive and without documented PD at the time of analysis were also censored at the date of their last disease assessment. Overall survival (OS) was defined as the time from the first study drug dose to the date of death from any cause. Subjects who were still alive at the data cutoff date were censored on the date they were last known to be alive. DOR was calculated as the time from the onset of response to the treatment to either disease progression or death for any reason. Changes in lymph node area and pharmacokinetic parameters were analyzed in all patients using the necessary baseline and on-study measurements. Statistical analysis was performed using GraphPad Prism 9.0 and STATA 15 software packages. Data were analyzed descriptively by dose regimen and histological subtype, as appropriate. Unless otherwise indicated, data from the dose-escalating and the dose-extension parts were combined for analysis.

3. Results

3.1. AI-assisted design of the brain-penetrant BTK inhibitor HZ-A-018

We initially designed and successfully optimized an AI model incorporating comprehensive molecular characterizations, including a Blood−Brain Barrier Penetration score (BBBp score) and a Killing score, for the rational design of novel BTK inhibitors (Fig. 1A−C, Supporting Information Fig. S1). Fig. 1A depicts the network architecture. The entire network was built using the PyTorch Geometric framework to predict BTK inhibitory activity and BBB permeability of compounds. The model architecture incorporates multiple graph attention layers to understand the significance of adjacent nodes within the molecular graph

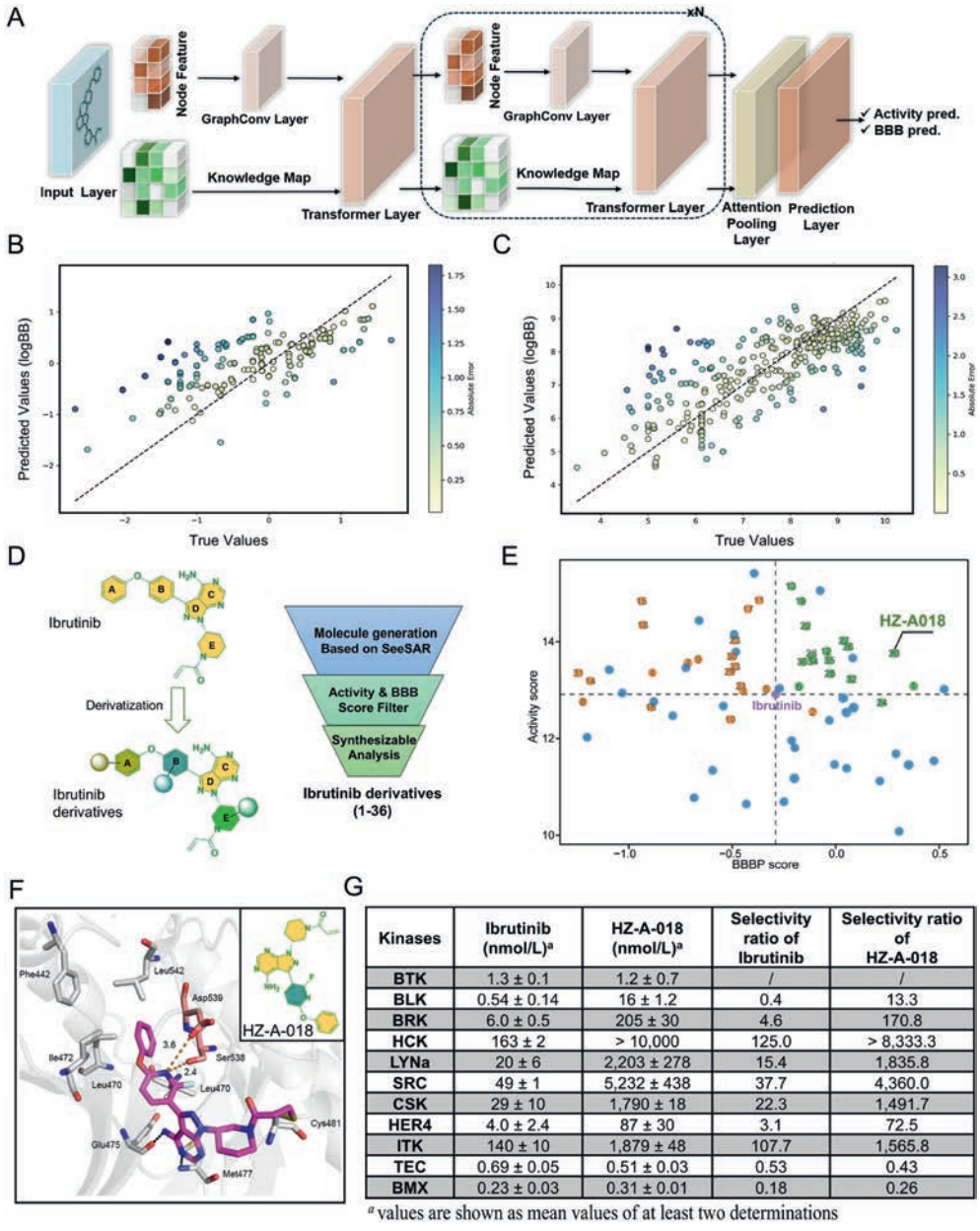

Kinases	Ibrutinib (nmol/L)[a]	HZ-A-018 (nmol/L)[a]	Selectivity ratio of Ibrutinib	Selectivity ratio of HZ-A-018
BTK	1.3 ± 0.1	1.2 ± 0.7	/	/
BLK	0.54 ± 0.14	16 ± 1.2	0.4	13.3
BRK	6.0 ± 0.5	205 ± 30	4.6	170.8
HCK	163 ± 2	> 10,000	125.0	> 8,333.3
LYNa	20 ± 6	2,203 ± 278	15.4	1,835.8
SRC	49 ± 1	5,232 ± 438	37.7	4,360.0
CSK	29 ± 10	1,790 ± 18	22.3	1,491.7
HER4	4.0 ± 2.4	87 ± 30	3.1	72.5
ITK	140 ± 10	1,879 ± 48	107.7	1,565.8
TEC	0.69 ± 0.05	0.51 ± 0.03	0.53	0.43
BMX	0.23 ± 0.03	0.31 ± 0.01	0.18	0.26

[a] values are shown as mean values of at least two determinations

Figure 1 Design and characterization of HZ-A-018. (A) The predictive model's architecture. (B) The performance of the BBBp score model on the test dataset. (C) The performance of the Killing score model on the test dataset. (D) Schematic illustration of the ibrutinib derivatives. (E) The BBBp and Killing scores of the generated ibrutinib derivatives were calibrated with ibrutinib (purple). (F) The binding mode of HZ-A-018 to BTK. (G) Kinase selectivity of HZ-A-018 and ibrutinib.

representation. Furthermore, the design includes a dense layer and a dropout layer at the end to improve prediction efficiency. This setup facilitates the focused aggregation of information from key neighboring nodes, enhancing the interpretation of intrinsic molecular characteristics. Then, a series of ibrutinib derivatives was generated using the SeeSAR Inspirator module and rational design guided by binding analysis of the ibrutinib/BTK complex (Fig. 1D, Supporting Information Table S1). Among these derivatives, HZ-A-018 emerged as the candidate with the optimal BBBp and Killing scores (Fig. 1E). Therefore, HZ-A-018 was synthesized for subsequent evaluation (Supporting Information Figs. S2 and S3).

To elucidate the binding mode and conformational stability of HZ-A-018, we performed a 50 ns molecular dynamics (MD) simulation on its complex with BTK kinase (PDB ID: 5P9J), following molecular docking. Upon stabilization of the RMSD values (Supporting Information Fig. S4), the 2-amino-pyrimidine moiety of HZ-A-018 generated strong H-bond interactions with Glu475 and Met477 in the hinge region of BTK (Fig. 1F). Subsequently, a biotin-labeled probe competitive ELISA was used to assess BTK occupancy by HZ-A-018 in human peripheral blood mononuclear cells (PBMCs) (Supporting Information Figs. S5−S7). The results showed that as the incubation concentration of HZ-A-018 increased, the BTK occupancy ratio

gradually increased, with an EC_{50} of 1.665 nmol/L (Supporting Information Fig. S8). The high BTK occupancy aligns with the characteristics of a covalent BTK inhibitor. Further kinase selectivity experiments showed HZ-A-018 outperformed ibrutinib in terms of BTK selectivity against a majority of the kinases selected for their importance in BTK selectivity research (Fig. 1G), and a comprehensive kinome analysis of HZ-A-018 encompassing a broad range of kinases was also performed (Supporting Information Fig. S9, Table S2).

3.2. HZ-A-018 demonstrates superior cytotoxicity and BBB penetration in vitro and in vivo

In the subsequent cytotoxicity assays, the cytotoxic effects of HZ-A-018 were significantly greater than those of tirabrutinib across all tested cell lines, particularly in human B-cell lymphoma cell lines TMD-8 and OCI-LY10, both of which overexpressed BTK [22,23] (Fig. 2A, Supporting Information Fig. S10). Moreover, Western blot analysis further validated that HZ-A-018 effectively suppressed BTK phosphorylation, with inhibition of the BTK pathway indicated by p-PLCγ2 and p-ERK (Fig. 2B, Supporting Information Fig. S11). Then, the MDCK-MDR1 model was used to assess the potential of compounds to penetrate the BBB [24,25]. HZ-A-018 exhibited substantially higher $P_{app(A-B)}$ values than ibrutinib and was equivalent to tirabrutinib, indicating its potential to cross the BBB (Fig. 2C, Supporting Information Table S3). This research furthermore tested the BBB-penetration capacity and *in vivo* antitumor activity of HZ-A-018. As shown in Fig. 2C, HZ-A-018 exhibited a notable brain C_{max}-to-plasma C_{max} (B/P) in the orthotopic mouse model, surpassing the values observed in the sham-operated group, with an enhanced B/P of HZ-A-018 compared with tirabrutinib in the orthotopic mouse model. This result suggests that HZ-A-018 has superior capability to penetrate the BBB and kill tumor cells in the mouse model. Additionally, pharmacokinetic (PK) evaluations in both SD rats and beagle dogs further confirmed the high oral bioavailability of HZ-A-018 (Supporting Information Table S4).

Building upon these comprehensive evaluations, we subsequently conducted an *in vivo* efficacy assessment of HZ-A-018 using an orthotopic CNS tumor model. The study first assessed the successful establishment of the orthotopic brain tumor model (Supporting Information Fig. S12) and then evaluated the ability of HZ-A-018 to cross the BBB and kill tumor cells. One day after Mino cell injection, all animals were randomly assigned to the HZ-A-018 (60 mg/kg, bid) treatment or vehicle groups. Then, we performed H&E, IHC, and mIF analyses to quantify tumor area and evaluate the change of BTK pathway in tumor cells after HZ-A-018 treatment for 3 weeks (Supporting Information Fig. S13 and S14). Quantitative analysis revealed a significant reduction in tumor area in the HZ-A-018-treated group compared with the vehicle group.

Furthermore, IHC analysis demonstrated elevated pBTK levels in tumor cells from the vehicle group, whereas representative regions from the HZ-A-018-treated group showed markedly diminished pBTK expression (Fig. S13B). To further establish the

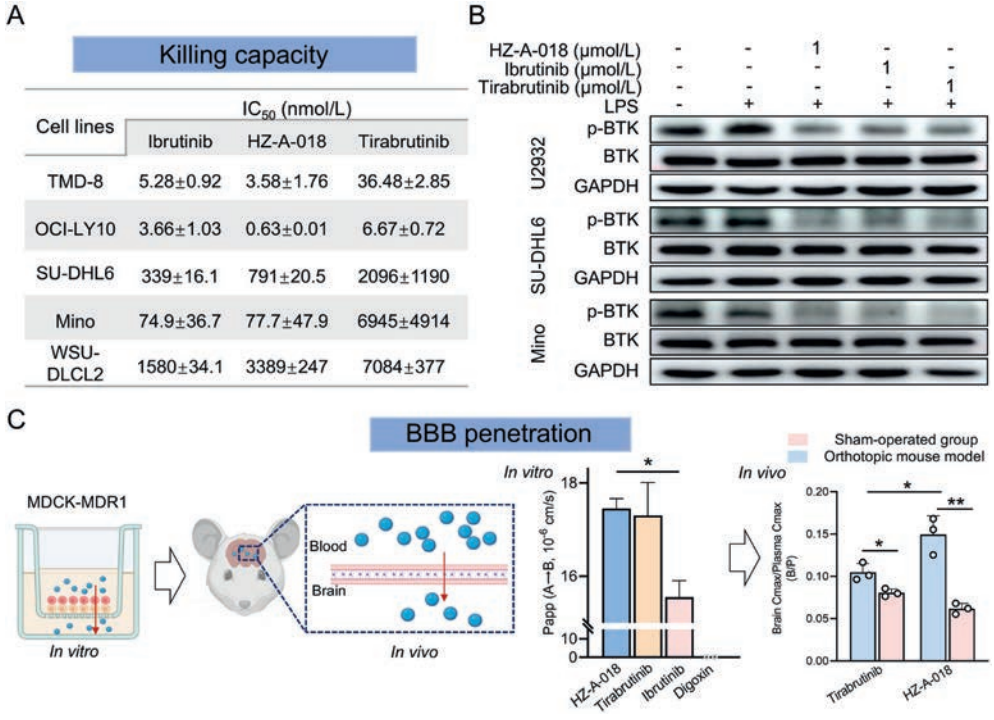

Figure 2 BTK inhibition, cytotoxicity, and BBB penetration of HZ-A-018. (A) Proliferation inhibitory effects of Ibrutinib, HZ-A-018, and tirabrutinib on various cell lines. The data shown are representative of more than two independent experiments. (B) Western blot analysis of BTK phosphorylation inhibition by Ibrutinib, HZ-A-018, or tirabrutinib in U2932, SU-DHL6, and Mino cells. (C) BBB permeability assessment of HZ-A-018 *in vitro* and *in vivo*. The P_{app} (A−B $\times$ 10^{-6} cm/s) values of Ibrutinib, HZ-A-018, and tirabrutinib are presented as mean ± SD. Statistical significance was determined using an ordinary one-way ANOVA with a Tukey's multiple comparisons test (*$P < 0.05$, $n = 2$ independent experiments). The B/P (brain tissue C_{max}/plasma C_{max}) of HZ-A-018 or tirabrutinib in sham-operated and orthotopic CB17 SCID mice is presented as mean ± SD ($n = 3$ independent experiments, *$P < 0.05$, **$P < 0.01$, two-tailed Student's *t*-test).

therapeutic advantage of HZ-A-018, mice were treated post-modeling with either ibrutinib (60 mg/kg) or HZ-A-018 (60 or 90 mg/kg) *via* oral gavage twice daily and monitored for survival ($n = 7$ per group) (Supporting Information Fig. S15A). The results showed that the treatment efficacy of the 60 and 90 mg/kg groups of HZ-A-018 was comparable, with both groups maintaining 100% survival at the time of treatment cessation (Fig. S15B). Both HZ-A-018 groups exhibited significantly better survival than the ibrutinib group.

3.3. Patients

Twenty-six patients (Table 1) with r/r CNSL were enrolled in the Phase Ia monotherapy study between February 2021 and December 2023 (Fig. 3). Overall, three patients were treated with HZ-A-018 300 mg, 12 with 450 mg, and 11 with 600 mg. With a data cutoff date of June 7, 2024, the median follow-up for the entire group was 30.0 months. The median follow-up for overall survival was 19.0 months, and 16 patients were still under follow-up.

The median age was 63.5 years (range, 36−80), and the median Karnofsky performance status (KPS) was 80 (range, 60−90). Twenty-three patients were diagnosed with PCNSL, and three had SCNSL. All patients had brain parenchymal lesions except for one PCNSL patient who presented with isolated intraocular involvement. Twelve patients experienced relapse, and fourteen patients had refractory disease. The median number of prior antitumor regimens was 1 (range, 1−4), including MTX-based chemotherapy (100%) and rituximab (92.3%). The baseline treatment characteristics of CNSL patients are shown in Table 1 and Supporting Information Table S5.

3.4. Safety

In the dose-escalation cohort, fifteen patients were assigned to the following dose levels: 300 mg ($n = 3$), 450 mg ($n = 6$), and 600 mg ($n = 6$). DLTs occurred in one patient each at the 450 mg and 600 mg dose levels: grade 4 neutropenia (450 mg) and grade 3 abnormal liver function (600 mg). However, the MTD was not reached at doses up to 600 mg. In the expansion cohort, six patients received 450 mg, and five received 600 mg. Overall, 12 patients (46.2%) experienced one or more treatment-related adverse events (TRAEs). The most frequent TRAEs were thrombocytopenia (38.5%), leukopenia (19.2%), neutropenia (19.2%), hyperbilirubinemia (11.5%), hypokalemia (11.5%), hyperuricemia (11.5%), and sinus bradycardia (11.5%) (Table 2). Grade ≥3 TRAEs occurred in five patients and included neutropenia (11.5%), leukopenia (3.8%), and abnormal liver function (3.8%).

A total of 10 patients experienced serious AEs, constituting 38.5% of the cohort, with three cases (11.5%) being treatment-related. Two patients discontinued HZ-A-018 due to AEs unrelated to the treatment. One patient in the 300 mg group experienced grade 3 cerebral edema, and one patient in the 450 mg group had grade 3 pulmonary artery embolism. No grade 5 AEs were observed.

Table 1 Baseline patient characteristics.

Baseline characteristics	300 mg ($N = 3$)	450 mg ($N = 12$)	600 mg ($N = 11$)	All ($N = 26$)
Age, median, y (range)	51 (36−62)	66 (39−80)	64 (50−70)	63.5 (36−80)
Sex, male, *n* (%)	1 (33.3)	9 (75.0)	7 (63.6)	17 (65.4)
Karnofsky performance status, median (range)	70 (70−80)	80 (60−90)	70 (60−90)	80 (60−90)
CNS lymphoma, *n* (%)				
Primary (PCNSL)	2 (66.7)	10 (83.3)	11 (100.0)	23 (88.5)
Secondary (SCNSL)	1 (33.3)	2 (16.7)	0 (0)	3 (11.5)
GCB subtype, *n* (%)				
GCB DLBCL	2 (66.7)	3 (25.0)	1 (9.1)	6 (23.1)
Non-GCB DLBCL	1 (33.3)	9 (75.0)	10 (90.9)	20 (76.9)
CNS involvement, *n* (%)				
Brain parenchyma	3 (100.0)	11 (91.7)	11 (100.0)	25 (96.2)
Intraocular[a]	0	1 (8.3)	0	1 (3.8)
CSF	0 (0)	0 (0)	0 (0)	0 (0)
Elevated LDH, *n* (%)	0 (0)	3 (25.0%)	2 (18.2)	5 (19.2)
Elevated CSF protein concentration, *n* (%)	2 (66.7)	6 (50.0)	2 (18.2)	10 (38.5)
Disease status, *n* (%)				
Relapse[b]	2 (66.7)	6 (50.0)	4 (36.4)	12 (46.2)
Refractory[c]	1 (33.3)	6 (50.0)	7 (63.6)	14 (53.8)
Prior treatment, *n* (%)				
MTX-based chemotherapy	3 (100.0)	12 (100.0)	11 (100.0)	26 (100.0)
Rituximab	3 (100.0)	11 (91.7%)	10 (90.9)	24 (92.3)
Radiation	0 (0)	1 (8.3%)	0 (0)	1 (3.8)
Number of prior regimens, median (range)	2 (1−2)	1 (1−3)	1 (1−4)	1 (1−4)
The sum of the greatest diameters at the target lesion, mm^2, *n* (%)				
<400	1 (33.3)	4 (36.3)	4 (36.4)	9 (36.0)
≥400	2 (66.7)	7 (63.6)	7 (63.6)	16 (64.0)
Median, mm^2 (range)	1929.2 (265.4−2769.2)	550.0 (148.8−2563.7)	620.2 (109.0−2545.9)	620.2 (109.0−2769.2)

[a]One PCNSL patient relapsed with an isolated intraocular lesion, without any target lesion in the brain parenchyma before entering this trial.
[b]A disease that responded to the last therapy (CR, CRu, or PR) but progressed afterward was defined as "relapse".
[c]A disease that did not respond to the last therapy (SD or PD) or was intolerant to it was defined as "refractory".

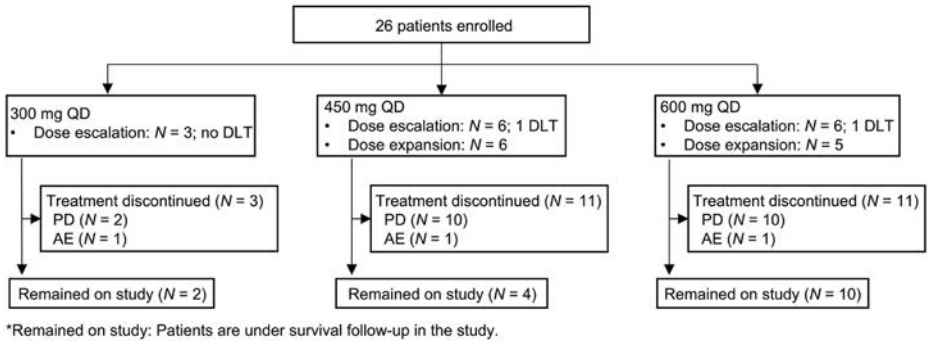

Figure 3 Patient disposition. AE, adverse event; PD, progressive disease.

Table 2 Treatment-related adverse events of any grade (frequency >5%).

Treatment-related adverse events	Grade 1–2 *N* (%)	Grade 3–4 *N* (%)	Total (*N* = 26) *N* (%)
Thrombocytopenia	10 (38.5)	0	10 (38.5)
Leukopenia	4 (15.4)	1 (3.8)	5 (19.2)
Neutropenia	2 (7.7)	3 (11.5)	5 (19.2)
Hyperbilirubinemia	3 (11.5)	0	3 (11.5)
Hypokalemia	3 (11.5)	0	3 (11.5)
Hyperuricemia	3 (11.5)	0	3 (11.5)
Sinus bradycardia	3 (11.5)	0	3 (11.5)
Abnormal liver function	1 (3.8)	1 (3.8)	2 (7.7)
Hypoproteinemia	2 (7.7)	0	2 (7.7)
Alanine aminotransferase increased	2 (7.7)	0	2 (7.7)
Rash	2 (7.7)	0	2 (7.7)
Nausea	2 (7.7)	0	2 (7.7)

3.5. *Efficacy*

Efficacy results were summarized in Table 3, with significant clinical responses observed across all dose levels (Fig. 4A, Supporting Information Fig. S16). The ORR was 50.0% (13/26), and the CRR was 19.2% (5/26). The ORR was 33.3% (1/3 patients) with no CR/CRu at 300 mg, 33.3% (4/12 patients) with two CR/CRu at 450 mg, and 72.7% (8/11 patients) with three CR/CRu at 600 mg.

With a median follow-up of 30.0 months, the Kaplan–Meier-estimated median progression-free survival (mPFS) was 1.91 months (95%CI: 1.8, 3.7) (Fig. 4B), while the median duration of response (mDOR) was 2.79 months (95%CI: 1.1, 2.9) among the 13 responders. After a median follow-up of 19.0 months, the Kaplan–Meier-estimated median overall survival (mOS) was not reached, and the 12-month survival rate was 66.5% (Fig. 4C). The mPFS was 1.91 months (95%CI: 1.9, NE) at 300 mg, 1.91 months at 450 mg (95%CI: 1.0, 16.8), and 3.15 months (95%CI: 0.8, 3.7) at 600 mg; the mDOR was 1.2 months at 450 mg (95%CI: 1.1, NE) and 2.79 months (95%CI: 1.0, 2.9) at 600 mg; the 12-month survival rate was 66.7% at 300 mg, 41.7% at 450 mg and 90.5% at 600 mg. MRI with T1-weighted contrast sequences demonstrated representative tumor response to HZ-A-018 in a PCNSL patient at 450 mg (#11) and a PCNSL patient at 600 mg (#16) (Fig. 4D).

3.6. *Pharmacokinetics*

Blood samples were collected during the steady-state phase from five patients in the 450 mg group and seven patients in the 600 mg group. HZ-A-018 demonstrated rapid absorption and elimination after oral administration at doses of 450 and 600 mg, with peak concentrations (C_{max}) occurring approximately 1.0–2.0 h post-dose at C3D1. Cerebrospinal fluid (CSF) samples were collected from five patients, revealing mean HZ-A-018 concentrations of 7.13 ng/mL (15.5 nmol/L) and 12.13 ng/mL (26.4 nmol/L) in the 450 and 600 mg groups, respectively (Supporting Information Fig. S17).

3.7. *Exploratory biomarker analyses*

We examined the relationship between clinical response to HZ-A-018 and the genotype of the tumor collected before treatment. The

Table 3 Efficacy summary in the r/r CNSL overall population (*N* = 26).

Endpoints	300 mg (*N* = 3)	450 mg (*N* = 12)	600 mg (*N* = 11)	All (*N* = 26)
Best ORR, *n* (%)	1 (33.3)	4 (33.3)	8 (72.7)	13 (50.0)
95% CI	0.8, 90.6	9.9, 65.1	39.0, 94.0	29.9, 70.1
Best CRR, *n* (%)	0 (0)	2 (16.7)	3 (27.3)	5 (19.2)
95% CI	0.0, 70.8	2.1, 48.4	6.0, 61.0	6.6, 39.4
Median PFS, months (95% CI)	1.91 (1.9, NE)	1.91 (1.0, 16.8)	3.15 (0.8, 3.7)	1.91 (1.8, 3.7)
Median DOR, months (95% CI)	NA	1.2 (1.1, NE)	2.79 (1.0, 2.9)	2.79 (1.1, 2.9)
Median OS, months (95% CI)	NE (15.4, NE)	9.0 (2.1, NE)	NE (NE, NE)	NE (9.0, NE)
12 months survival rate (95% CI), %	66.7 (5.4, 94.5)	41.7 (15.3, 66.5)	90.5 (49.1, 98.6)	66.5 (43.8, 81.8)

ORR=CR + CRu + PR; CR, complete response; CRR, complete response rate; CRu, unconfirmed complete response; PR, partial response; PFS, progression-free survival; OS, overall survival; NA, not available; NE, not evaluable.

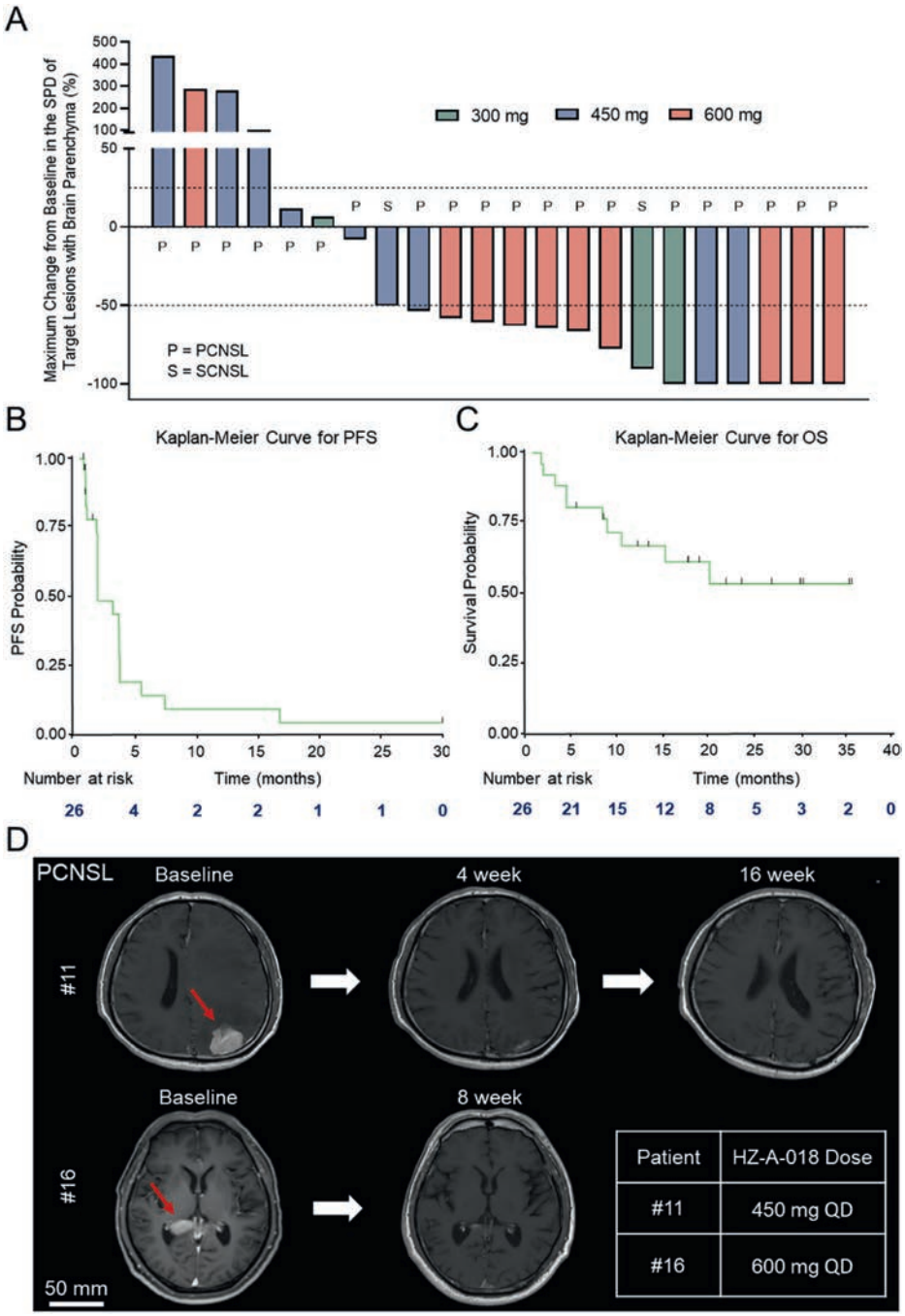

Figure 4 Clinical response to HZ-A-018 in r/r CNSL. (A) Maximum change in the SPD with brain lesions ($N = 22$). (B) Kaplan−Meier plot of PFS. (C) Kaplan−Meier plots of OS. (D) Representative tumor response to HZ-A-018, as determined by MRI contrast sequences, in PCNSL patients (#11 and #16).

tumor genotypes of seven patients were analyzed using next-generation sequencing (NGS); the results are shown in Supporting Information Table S6.

4. Discussion

CNSL is a rare and aggressive extranodal non-Hodgkin lymphoma with limited treatment options and no standard treatment, particularly for patients with relapsed or refractory disease [1,6,26]. Various agents have been investigated, but with limited response and survival. For example, the mTOR inhibitor temsirolimus has an ORR of 54%, with mPFS of 2.1 months and mOS of 3.7 months [27]. Topotecan [28] and temozolomide [29] have shown ORRs of 33% and 31%, with mPFS of 2.0 months and 2.8 months, and mOS of 8.4 and 3.9 months, respectively. BTK inhibitors have shown moderate responses for treating r/r CNSL, such as ibrutinib and tirabrutinib monotherapy. In the iLOC study, ibrutinib was administered at the approved dose of 560 mg, with an ORR of 47% and CRR of 10% in evaluable patients with brain lesions

($N = 30$), alongside a mPFS of 2 months (95% CI: 2−3) and a mOS of 4.3 months (95% CI: 3−9) [30,31]. Tirabrutinib was approved for treating r/r PCNSL in Japan, and in the phase I/II study, the ORR and CRR were 52.9% and 35.3%, respectively, in the 480 mg qd (fasted) cohort ($N = 17$), alongside an mPFS of 5.8 months (95% CI: 1.0−5.8) and mOS not reached [12]. Consequently, therapeutic options for CNSL remain limited. Although BTK inhibitors have demonstrated clinical efficacy, the current available agents is narrow.

What strategies can enhance the throughput in CNS antitumor drug development? One of the key challenges in CNS antitumor drug discovery is to simultaneously achieve drug penetration across the BBB and exert potent cytotoxicity against tumor cells. We have successfully developed an innovative BTK inhibitor HZ-A-018 for PCNSL treatment based on our comprehensive CNS drug prediction system. This study further evaluates the safety, tolerability, efficacy, and pharmacokinetics of HZ-A-018 monotherapy in elderly patients with r/r CNSL, for whom limited treatment alternatives are available in China. Regarding the safety profile, the most frequent TRAEs were thrombocytopenia (38.5%), leukopenia (19.2%), neutropenia (19.2%), hyperbilirubinemia (11.5%), hypokalemia (11.5%), hyperuricemia (11.5%), and sinus bradycardia (11.5%). Notably, only five patients (19.2%) experienced TRAEs of grade 3 or higher, with neutropenia being the most common. Furthermore, no grade 5 AEs were reported. Although a higher incidence of thrombocytopenia was observed with HZ-A-018 compared to tirabrutinib, which may be related to differences in the kinase selectivity profiles between the two agents, HZ-A-018 demonstrated a lower incidence of grade $\geq$3 thrombocytopenia. In addition, no cases of grade 3 or higher major hemorrhage or skin disorders were observed, indicating a favorable safety profile for the treatment.

Regarding efficacy, HZ-A-018 demonstrated remarkable survival outcomes, but with relatively limited PFS and duration of response. Specifically, in the 600 mg group, patients achieved an ORR of 72.7%, a mPFS of 3.15 months (95% CI: 0.8, 3.7), and a 12-month survival rate of 90.5%. These findings further supported the selection of the 600 mg dose as the RP2D. To our knowledge, PCNSL is a highly aggressive lymphoma with a relatively short PFS compared with indolent lymphomas. This is particularly evident in patients with relapsed or refractory disease, where the disease progresses rapidly, and OS may be limited to just a few months without treatment. The observed discrepancy in mPFS compared with tirabrutinib may be attributed to several factors. These include the intrinsically aggressive nature of PCNSL, the non-head-to-head design, and differences in patient baseline characteristics, such as the higher proportion of refractory disease in this study (53.8%) compared with the tirabrutinib trial (35%). According to various studies, the mOS for relapsed PCNSL patients is only 3.5 to 4.5 months, with refractory patients faring worse, with an mOS of only 2 months. Based on our research findings, we suppose that using HZ-A-018 in r/r PCNSL has significantly improved disease response rates, delayed progression, and survival outcomes. Additionally, HZ-A-018 treatment enhances patients' tolerance to subsequent therapies, predominantly salvage chemotherapy, thereby improving their overall quality of life. The details of the following treatment regimens have been provided in Supporting Information Table S7.

Simultaneously, analysis of plasma and cerebrospinal fluid (CSF) samples collected 2 h after HZ-A-018 administration confirmed its BBB penetration (Fig. S17). However, HZ-A-018 did not exceed tirabrutinib in drug exposure within the human brain[12]. Potential reasons include the lower plasma protein binding of tirabrutinib compared to HZ-A-018 (Supporting Information Table S8). Meanwhile, the species-specific differences in BBB penetration between the two drugs could be due to their distinct plasma protein-binding profiles and the quantification methods (brain homogenate *vs.* CSF). This requires further exploration. This finding nevertheless underscores, to some extent, the importance of our dual-parameter model that integrates both BBB penetration capability and tumor cell killing potency, as the comprehensive performance ultimately dictates the therapeutic efficacy of this class of drugs. In fact, the ORR of HZ-A-018 at 600 mg was 72.7%, numerically higher than ibrutinib (47%) and tirabrutinib (52.9%) at their recommended target doses. The mOS of ibrutinib was 4.3 months, and the mOS of tirabrutinib was not reached. However, the inherent limitations in the above comparisons necessitate that the results be interpreted with caution and regarded as preliminary. Preliminary clinical efficacy data suggest that HZ-A-018 may possess superior therapeutic potential for CNS lymphoma, though further validation in subsequent clinical studies is required.

In addition, *MYD88*, *CD79B*, and *CARD11* mutations were identified in five out of six PCNSL cases (Table S6). Two patients harbored mutations in all three genes—*MYD88*, *CD79B*, and *CARD11*—and achieved complete response (CR) with CR duration exceeding 12 months. However, given the limited sample size in this study, further clinical investigations with larger cohorts are needed to better understand the relationships between key oncogenic mutations and treatment response. Meanwhile, this study enrolled only one patient with intraocular disease and none with meningeal dissemination. In the following phase II trial, we plan to expand the biomarker analysis to include more patients for validation, thereby enabling a more robust analysis. Furthermore, although all enrolled patients had previously received HD-MTX-based chemotherapy, and 92.3% had received rituximab, none received autologous stem cell transplantation as consolidation therapy. The limited availability of thiotepa and prevailing economic constraints led to comparatively low transplantation rates in this study, potentially overestimating of the efficacy of salvage therapy.

The successful preclinical and clinical development of innovative molecules based on the AI predictive model in this study suggests that this integrated BBB penetration and cytotoxicity prediction system may not only facilitate the discovery of BTK inhibitors for CNS lymphoma but could potentially be extended to research targeting other related targets of brain diseases. Future studies employing this paradigm to predict BBB-penetrant cytotoxic molecules, to conduct clinical investigations, and to expand therapeutic indications would likely be warranted.

5. Conclusions

In this study, we developed a dual-parameter prediction model integrating blood−brain barrier (BBB) penetration and cytotoxic potency, which guided the discovery of the novel BTK inhibitor HZ-A-018 for the treatment of central nervous system lymphoma. HZ-A-018 has demonstrated favorable safety and remarkable efficacy, achieving high response rates and significantly prolonging patients' survival. Based on phase Ia safety and efficacy data from the HZ-A-018-102 study, HZ-A-018 has been granted breakthrough therapy designation by China's National Medical Products Administration (NMPA) for the treatment of relapsed/refractory primary CNS lymphoma (r/r PCNSL). The Center for

Drug Evaluation (CDE) in China has authorized initiation of a single-arm phase II registrational trial as a pivotal study for accelerated approval of HZ-A-018 monotherapy in r/r PCNSL patients. Further validation studies are warranted to determine the applicability of this paradigm across a broader spectrum of CNS disorders.

Acknowledgments

This work was funded by HealZen Therapeutics Co., Ltd., Hangzhou, China. All schematics were created using BioRender (www.biorender.com).

Author contributions

Wenbin Li, Xiaowu Dong, and Feng Chen contributed to the conception and design. Shenglan Li, Zhuang Kang, Haiyan Yang, Wenbin Qian, Xi Chen, and Xianggui Yuan collected clinical data. Miao Hu, Zhuang Kang, and Feng Chen performed statistical analysis and interpreted data. Jialiang Lu and Qiuqiu Shi conducted preclinical research. Shenglan Li, Jialiang Lu, Zhuang Kang, Miao Hu, and Xinglu Zhou drafted the manuscript. Wenbin Li, Xiaowu Dong, and Feng Chen checked the manuscript. All authors have read and approved the article. Shenglan Li, Jialiang Lu, and Zhuang Kang contributed equally to this study.

Conflicts of interest

Xiaowu Dong and Xinglu Zhou are co-founders of HealZen Therapeutics Co., Ltd., and Miao Hu is an employee of HealZen Therapeutics Co., Ltd. The other authors declare no conflict of interest.

Appendix A. Supporting information

Supporting information to this article can be found online at https://doi.org/10.1016/j.apsb.2026.05.021.

References

1. Ferreri AJM, Calimeri T, Cwynarski K, Dietrich J, Grommes C, Hoang-Xuan K, et al. Primary central nervous system lymphoma. *Nat Rev Dis Primers* 2023;**9**:29.
2. Ferreri AJ, Reni M, Villa E. Therapeutic management of primary central nervous system lymphoma: lessons from prospective trials. *Ann Oncol* 2000;**11**:927−37.
3. Duan L, Guo W, Yin S, Yang S, Liu J, Duan Y, et al. The baseline pan-immune-inflammation value (PIV) and PILE in predicting clinical outcomes and therapeutic response for primary central nervous system lymphoma. *J Inflamm Res* 2024;**17**:5347−63.
4. Okita Y, Kano-Fujiwara R, Nakatsuka SI, Honma K, Kinoshita M. Histological verification of the treatment effect of tirabrutinib for relapsed/refractory primary central nervous system lymphoma. *Exp Hematol Oncol* 2021;**10**:29.
5. Stanchina MD, Montoya S, Danilov AV, Castillo JJ, Alencar AJ, Chavez JC, et al. Navigating the changing landscape of BTK-targeted therapies for B cell lymphomas and chronic lymphocytic leukaemia. *Nat Rev Clin Oncol* 2024;**21**:867−87.
6. Patrij K, Reiser M, Wätzel L, Pels H, Kowoll A, Herrlinger U, et al. Isolated central nervous system relapse of systemic lymphoma (SCNSL): clinical features and outcome of a retrospective analysis. *Ger Med Sci* 2011;**9**:Doc11.
7. Epperla N, Feng L, Shah NN, Fitzgerald L, Shah H, Stephens DM, et al. Outcomes of patients with secondary central nervous system lymphoma following CAR T-cell therapy: a multicenter cohort study. *J Hematol Oncol* 2023;**16**:111.
8. Alderuccio JP, Nayak L, Cwynarski K. How I treat secondary CNS involvement by aggressive lymphomas. *Blood* 2023;**142**: 1771−83.
9. Calimeri T, Steidl C, Fiore P, Ferreri AJM. New hopes in relapsed refractory primary central nervous system lymphoma. *Curr Opin Oncol* 2023;**35**:364−72.
10. Losi G, Mussetti A, Peña M, Lopez-Pereira P, Sureda A, Novelli S. Anti-CD19 CAR T-cell therapy for primary and secondary CNS lymphomas. *Bone Marrow Transplant* 2025;**60**:259−69.
11. Walter HS, Rule SA, Dyer MJ, Karlin L, Jones C, Cazin B, et al. A phase 1 clinical trial of the selective BTK inhibitor ONO/GS-4059 in relapsed and refractory mature B-cell malignancies. *Blood* 2016;**127**:411−9.
12. Narita Y, Nagane M, Mishima K, Terui Y, Arakawa Y, Yonezawa H, et al. Phase I/II study of tirabrutinib, a second-generation Bruton's tyrosine kinase inhibitor, in relapsed/refractory primary central nervous system lymphoma. *Neuro Oncol* 2021;**23**:122−33.
13. Yu H, Kong H, Li C, Dong X, Wu Y, Zhuang Y, et al. Bruton's tyrosine kinase inhibitors in primary central nervous system lymphoma-evaluation of antitumor efficacy and brain distribution. *Transl Cancer Res* 2021;**10**:1975−83.
14. Neuwelt E, Abbott NJ, Abrey L, Banks WA, Blakley B, Davis T, et al. Strategies to advance translational research into brain barriers. *Lancet Neurol* 2008;**7**:84−96.
15. Rosa LCS, Argolo CO, Nascimento CMC, Pimentel AS. Identifying substructures that facilitate compounds to penetrate the blood−brain barrier *via* passive transport using machine learning explainer models. *ACS Chem Neurosci* 2024;**15**:2144−59.
16. Singh AV, Chandrasekar V, Janapareddy P, Mathews DE, Laux P, Luch A, et al. Emerging application of nanorobotics and artificial intelligence to cross the BBB: advances in design, controlled maneuvering, and targeting of the barriers. *ACS Chem Neurosci* 2021;**12**:1835−53.
17. Huang ETC, Yang JS, Liao KYK, Tseng WCW, Lee CK, Gill M, et al. Predicting blood−brain barrier permeability of molecules with a large language model and machine learning. *Sci Rep* 2024;**14**:15844.
18. Guo Y, Shen Z, Zhao W, Lu J, Song Y, Shen L, et al. Rational identification of novel antibody−drug conjugate with high bystander killing effect against heterogeneous tumors. *Adv Sci (Weinh)* 2024;**11**: e2306309.
19. Gao J, Shen Z, Xie Y, Lu J, Lu Y, Chen S, et al. TransFoxMol: predicting molecular property with focused attention. *Briefings Bioinf* 2023;**24**:bbad306.
20. Gao J, Shen Z, Lu Y, Shen L, Zhou B, Xu D, et al. KnoMol: a knowledge-enhanced graph transformer for molecular property prediction. *J Chem Inf Model* 2024;**64**:7337−48.
21. Abrey LE, Batchelor TT, Ferreri AJ, Gospodarowicz M, Pulczynski EJ, Zucca E, et al. Report of an international workshop to standardize baseline evaluation and response criteria for primary CNS lymphoma. *J Clin Oncol* 2005;**23**:5034−43.
22. Song X, Rao H, Guo C, Yang B, Ren Y, Wang M, et al. Myricetin exhibit selective anti-lymphoma activity by targeting BTK and is effective *via* oral administration *in vivo*. *Phytomedicine* 2021;**93**: 153802.
23. Chen Y, Bai G, Ning Y, Cai S, Zhang T, Song P, et al. Design and synthesis of Imidazo[1,2-*b*]pyridazine IRAK4 inhibitors for the treatment of mutant MYD88 L265P diffuse large B-cell lymphoma. *Eur J Med Chem* 2020;**190**:112092.
24. Gupta M, Feng J, Bhisetti G. Experimental and computational methods to assess central nervous system penetration of small molecules. *Molecules* 2024;**29**:1264.
25. Wu VM, Huynh E, Tang S, Uskoković V. Brain and bone cancer targeting by a ferrofluid composed of superparamagnetic iron-oxide/silica/carbon nanoparticles (earthicles). *Acta Biomater* 2019;**88**:422−47.
26. Schaff LR, Grommes C. Primary central nervous system lymphoma. *Blood* 2022;**140**:971−9.

27. Korfel A, Schlegel U, Herrlinger U, Dreyling M, Schmidt C, von Baumgarten L, et al. Phase II trial of temsirolimus for relapsed/refractory primary CNS lymphoma. *J Clin Oncol* 2016;**34**:1757−63.
28. Fischer L, Thiel E, Klasen HA, Birkmann J, Jahnke K, Martus P, et al. Prospective trial on topotecan salvage therapy in primary CNS lymphoma. *Ann Oncol* 2006;**17**:1141−5.
29. Reni M, Zaja F, Mason W, Perry J, Mazza E, Spina M, et al. Temozolomide as salvage treatment in primary brain lymphomas. *Br J Cancer* 2007;**96**:864−7.
30. Soussain C, Malaise D, Choquet S, Ghesquières H, Houillier C. Long-lasting CRs after ibrutinib monotherapy for relapse or refractory primary CNS lymphoma (PCNSL) and primary vitreoretinal lymphoma (PVRL): long-term results of the iLOC study by the lymphoma study association (LYSA) and the French oculocerebral lymphoma (LOC) network (clinical trial number: NCT02542514). *Eur J Cancer* 2023;**189**:112909.
31. Soussain C, Choquet S, Blonski M, Leclercq D, Houillier C, Rezai K, et al. Ibrutinib monotherapy for relapse or refractory primary CNS lymphoma and primary vitreoretinal lymphoma: final analysis of the phase II proof-of-concept' iLOC study by the Lymphoma study association (LYSA) and the French oculo-cerebral lymphoma (LOC) network. *Eur J Cancer* 2019;**117**:121−30.